SINTECHCOM: Science, Technology and Communication Journal
Vol. 7, No. 1, October 2026, pp. 25-36, DOI: 10.59190/stc.v7i1.436

High-energy supercapacitor based on phosphoric acid (H_3PO_4)-activated *Moringa oleifera* leave waste as the electrode material

Salma Safitri[1], Fitriani Novalina Panjaitan[1], Novi Yanti[1], Nursyafni Nursyafni[1], Apriwandi Apriwandi[1], Rika Taslim[2], Erman Taer[1,*]
[1]Department of Physics, Universitas Riau, Pekanbaru 28293, Indonesia
[2]Department of Industrial Engineering, UIN Sultan Syarif Kasim Riau, Pekanbaru 28293, Indonesia

ABSTRACT

Moringa oleifera-leaves were used as the main starting material for making activated carbon for supercapacitor electrodes. The research focused on producing *Moringa oleifera*-leaves activated carbon and examining its physical properties and electrochemical performance. The activated carbon was produced through a chemical activation process using 0.5 M H_3PO_4, carbonization under N_2 gas, and physical activation using CO_2 gas. Density measurements showed a decrease from 0.94 g/cm^3 to 0.60 g/cm^3 following pyrolysis, representing a reduction of 36.17%. Electrochemical testing was performed using cyclic voltammetry (CV) and galvanostatic charge–discharge (GCD) methods in a 1 M Na_2SO_4 electrolyte with a current density of 1 A/g. Results obtained within a test voltage window of 0 – 1 V yielded specific capacitances of 45 F/g (CV) and 130 F/g (GCD). Further testing across a wider operating voltage window of 0 – 2 V resulted in a specific capacitance of 153.33 F/g, with a specific energy of 85.18 Wh/kg, and specific power of 1,840 W/kg. These findings demonstrate the potential of *Moringa oleifera* leaves waste for use as an electrode material in supercapacitors capable of operating at a voltage range of 0 – 2 V, thereby supporting the development of high-energy supercapacitors.

ARTICLE INFO

Article history:

Received Aug 21, 2026
Revised Sep 28, 2026
Accepted Oct 5, 2026
Published Oct 30, 2026

Keywords:

Activated Carbon
Electrode Material
Moringa oleifera
Supercapacitor
Waste

Copyright (c) 2026:

Salma Safitri, Fitriani Novalina Panjaitan, Novi Yanti, Nursyafni, Apriwandi, Rika Taslim, Erman Taer

License:

This work is licensed under a Creative Commons Attribution 4.0 International License (CC BY).

*Corresponding Author
E-mail address: erman.taer@lecturer.unri.ac.id

1. INTRODUCTION

Supercapacitors can store and release charge rapidly while maintaining their performance over repeated cycles, making them widely developed as electrochemical energy storage devices. Their advantage lies in delivering high power; However, the amount of energy that supercapacitors can store remains one of the limitations in their development. Efforts to improve energy storage capability are not only related to improving the materials used for electrodes but also involve adjustment of cell operating conditions. One operating condition that needs to be considered is the voltage applied during

supercapacitor operation. Increasing the voltage may significantly affect the amount of energy stored [1]. However, the use of high voltages in aqueous systems requires consideration of electrolyte and electrode stability because it may trigger water decomposition reactions [2]. One material widely used as a supercapacitor electrode is porous carbon, as its surface and pores provide sites for charge storage and interactions with electrolyte ions. Pore size affects ion accessibility, while the surface area and pore volume are related to portion of the carbon surface utilized during the charge storage process.

Biomass has been explored as a raw material in the production of activated carbon has become one approach in electrode material development because it provides a renewable carbon source [3]. One type of biomass with potential for this purpose is moringa leaves (*Moringa oleifera*) [4]. The development of *Moringa oleifera* leave-based carbon has also demonstrated electrochemical characteristics that support its application as an electric double-layer capacitor (EDLC) electrode [5]. *Moringa oleifera* leave-based carbon electrodes have previously been reported by [4] using ZnCl impregnation, carbonization in an N_2 atmospheric gas, followed by physical activation under CO_2 gas at a temperature range of 650 to 850°C. The results showed that the specific surface area (SSA) increased from 211.334 m^2/g at 650°C to 412.196 m^2/g at 750°C, before decreasing to 322.008 m^2/g at 850°C. These findings indicate that the activation temperature affects the development of the pore structure in *Moringa oleifera* leave-based carbon [5]. Variations in carbonization temperature can affect the surface morphology and pore distribution of carbon, which are related to its specific surface area and electrochemical performance [6]. Pore structure development can also be achieved through chemical activation using H_3PO_4, which influences modifications to the material structure and the surface properties of carbon [4]. The use of 0.5 M H_3PO_4 and $ZnCl_2$ as chemical treatments has been reported to produce a two-dimensional (2D) nanosheet-nanofiber structure integrated with a three-dimensional (3D) hierarchical pore network. The resulting carbon had an oxygen content of 17.62% and achieved a capacitance per unit mass reaching 201 F/g when tested in a 1 M H_2SO_4 solution, with a maximum energy density of 25 Wh/kg at a power density of 122 W/kg.

Beyond its electrochemical performance, the use of *Moringa oleifera* leave waste offers an opportunity to add value to underutilized biomass and support the development of more sustainable energy-storage materials. Converting this residue into activated carbon may help reduce biomass disposal and reliance on conventional carbon precursors. However, the overall environmental benefits depend on the resources required for chemical activation, carbonization, and physical activation. Assessing these factors is therefore important for determining the sustainability of the production process.

In addition to electrode characteristics, the electrolyte is also one of the factors affecting supercapacitor performance because the ions in the electrolyte play a role in charge transfer at the electrode surface. Aqueous electrolytes are widely used because they offer high ionic conductivity, relatively low cost, non-flammability, and greater safety compared with several other types of electrolytes [1]. The properties of the electrolyte are also related to the energy, power, cycle stability, and efficiency of supercapacitor devices [7]. Ionic conductivity affects ion transport and resistance within the cell, while concentration and temperature can alter ion transport properties in the solution [8]. Furthermore, electrolyte characteristics help determine electrochemical stability and the operating voltage window that can be used in aqueous supercapacitors [2].

One aqueous electrolyte that can be used in carbon-based systems is Na_2SO_4 because it is neutral and can be used under operating conditions within a voltage range of 0 – 2 V compared with several other aqueous electrolytes. Its neutral nature can improve resistance to hydrogen and oxygen evolution reactions under certain conditions [9]. The performance of the Na_2SO_4 electrolyte is also influenced by solution concentration, as changes in concentration can affect electrolyte conductivity and resistance [10]. This concentration effect is related to the number of ions available to carry charge in the solution and the ability of the ions to move toward the electrode surface [8]. In addition, ionic characteristics and their interactions with the electrolyte environment can influence ion transport into carbon pores [7].

Using water-based electrolytes at high voltages still has limitations because water can undergo decomposition reactions, producing hydrogen at the negative electrode and oxygen at the positive electrode [1]. Thermodynamically, water decomposition is associated with a potential of approximately 1.23 V; however, the actual voltage limit of a cell may depend on the electrode material, the electrolyte composition, polarization, and the conditions at the electrode–electrolyte interface [2]. Extending

the operating voltage window is one strategy to increase the specific energy density of aqueous supercapacitor systems; therefore, choosing suitable electrode materials and electrolytes needs to be considered simultaneously [11]. However, a higher electrolyte concentration does not necessarily always produce similar results, as the electrolyte conditions and electrode materials determine the resulting electrochemical response [10]. Therefore, the suitability of the 0 – 2 V voltage window for *Moringa oleifera* leave-derived activated carbon in 1 M Na_2SO_4 was investigated in terms of its electrochemical energy-storage performance.

The novelty of this study is the use of H_3PO_4 chemical activation followed by CO_2 physical activation to produce *Moringa oleifera* leave-derived activated carbon, as an alternative to the $ZnCl_2$ based chemical activation followed by CO_2 physical activation reported in previous work [5]. In addition, this study investigates the effect of expanding the CV voltage window from 0 – 1 V to 0 – 2 V using a 1 M Na_2SO_4 electrolyte on the electrode's specific capacitance, energy density, and power density.

2. RESEARCH METHODS

The overall preparation process of *Moringa oleifera* leaves-based activated carbon electrodes and their electrochemical characterization is illustrated in Figure 1.

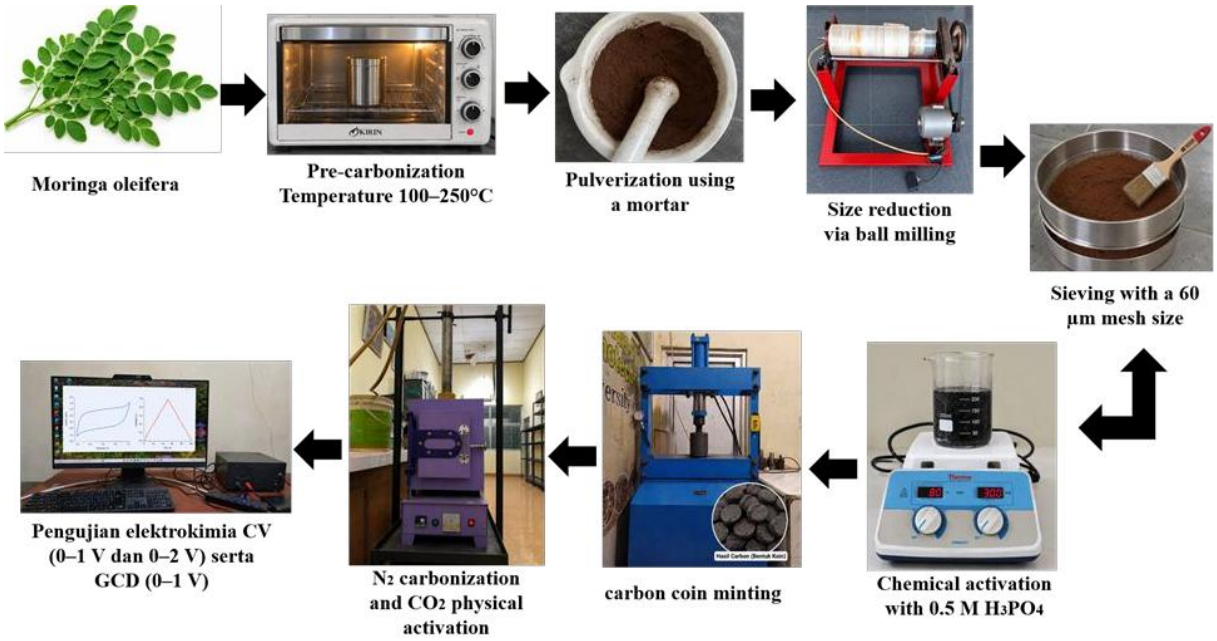


Figure 1. Schematic workflow of the experimental procedure.

Moringa oleifera leaves-carbon precursors were separated from the stems and petioles, then rinsed with clean water to remove any dirt or impurities from the surface contaminants. The samples were sun-dried for 48 hours until they became dry and yellowish in color. Subsequently, 30 g of the dried samples was weighed for pre-carbonization in a vacuum oven for 2 hours, with gradual heating from 100°C to 250°C. The resulting brittle samples were ground using a mortar and ball mill for 24 hours, with an operating cycle of 4 hours followed by a 1-hour rest period. The samples were then sieved through a 60 µm mesh to achieve a uniform particle size. The chemical activation process was performed with a 0.5 M solution of H_3PO_4. This solution was made by mixing 8.5 ml of H_3PO_4 with 250 ml of distilled water before adding 50 g of carbon powder. Chemical activation was carried out using a hot plate at 80°C with a stirring speed of 300 rpm for a total of 3 hours. The activated samples were oven-dried for 3 days, then ground using a mortar and sieved again before pelletization. The carbon powder was pressed into pellets with a hydraulic press under a pressure of 8 tons for 2 minutes. The coin-shaped carbon pellets were placed in a furnace for the carbonization and activation stages. Heating began with heating from 30°C to 600°C at a heating rate of 1°C/min in an N_2 atmospheres for

7.2 hours to facilitate carbonization. The process was followed by physical activation with CO_2 gas, with the temperature increased from 600°C to 750°C at 10°C/min and held at 750°C for 2.5 hours. The resulting activated carbon pellets were washed in 500 ml of distilled water over a period of 5 – 7 days until the pH reached 7. The activated carbon pellets were dried in an oven and then sanded using P600-grit sandpaper to adjust the diameter and P1200-grit sandpaper to adjust the thickness, producing electrodes measuring 7 – 8 mm in diameter and 0.2 – 0.3 mm in thickness. The electrodes were afterwards immersed in a 1 M solution of Na_2SO_4 for 2 days to promote electrolyte penetration and accumulation within the electrode pores. The electrode, separator, current collector, and electrolyte components were assembled into a supercapacitor cell to evaluate its capacitive performance using the galvanostatic charge–discharge (GCD) and cyclic voltammetry (CV) techniques. GCD measurements were performed with a CD UR Red-ER 2018 instrument at a potential range of 0 – 1 V, while CV measurements were conducted with a Physics CV UR Rad-ER 5841 instrument at voltage ranges of 0 – 1 V and 0 – 2 V to investigate changes in current response as a function of voltage. Each electrochemical test was performed single for each testing condition.

3. RESULTS AND DISCUSSIONS

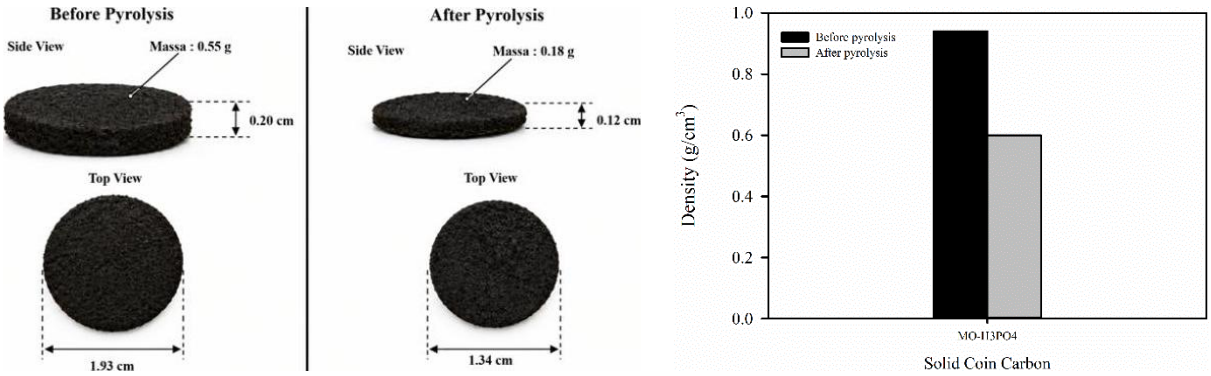
3.1. Physical Characterization

3.1.1. Density Analysis

Density measurements were performed to determine changes in the physical properties of *Moringa oleifera* leaves-based activated carbon electrodes after thermal treatment involving carbonization under an N_2 atmosphere and physical activation using CO_2 gas. The following equation was used to calculate density, as shown in Equation (1):

$$\rho = \frac{m}{V} \tag{1}$$

where ρ represents density (g/cm^3), m represents mass (g), and V represents volume (cm^3) [12].



(a) (b)

Figure 2. Physical changes in the pellest (a) and density comparison (b) before and after pyrolysis.

Based on Figure 2 (a), physical changes in the pellet can be observed before and after pyrolysis. The pellet mass decreased from 0.55 g to 0.18 g, while its diameter decreased from 1.93 cm to 1.34 cm and its thickness decreased from 0.20 cm to 0.12 cm. These changes indicate that the pyrolysis process affected the mass and dimensions of the pellet. The mass reduction can be attributed to the release of volatile compounds during heating, while the changes in diameter and thickness indicate material shrinkage. These physical changes demonstrate that thermal treatment affects the characteristics of the resulting pellet.

Figure 2 (b) shows that the density of *Moringa oleifera* leaves-based carbon decreased from 0.94 g/cm^3 before pyrolysis to 0.60 g/cm^3 after pyrolysis, representing a reduction of 36.17%. This

decrease indicates changes in the physical properties of the material following thermal treatment. These changes are associated with the decomposition of lignocellulosic components, including cellulose, hemicellulose, and lignin, during heating, accompanied by the release of volatile compounds [13]. The release of these components reduces the material mass and alters the characteristics of the carbon produced from the initial precursor [14].

In addition, the density change may also be influenced by the use of H_3PO_4 as a chemical activating agent. The interaction of H_3PO_4 with biomass components can affect carbon formation and the amount of solid material remaining after treatment [15]. These changes may influence the material characteristics and the mass-to-volume ratio [16]. Further changes may occur during physical activation using CO_2 at 750°C. Under these conditions, CO_2 can react with carbon to produce gaseous products, resulting in a reduction in carbon mass. Mass loss during activation can affect the final material density, while the extent of this change depends on activation conditions, including temperature and treatment duration [17]. Therefore, the combined treatments of chemical activation using H_3PO_4 and physical activation using CO_2 can influence the physical characteristics of the resulting carbon.

3.2. Electrochemical Characterization

3.2.1. Galvanostatic Charging and Discharging Analysis

GCD testing was conducted to evaluate the ability of *Moringa oleifera* leaves-based activated carbon electrodes to store and release charge under constant-current conditions. The test monitors voltage changes over time throughout charging and discharging, which indicates the electrode's capacitive response characteristics [18].

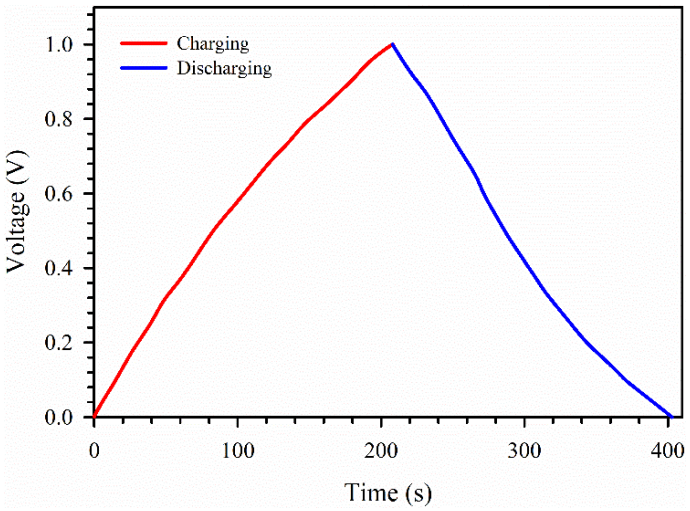


Figure 3. GCD curve at a voltage of 1 V.

Based on Figure 3, the charging process occurs between 0 V and 1 V for 205 s, followed by discharging from 1 V to 0 V for 195 s. The curve exhibits a relatively regular pattern, with a shape that approaches a triangle with a slight slope [19]. This response is influenced by the use of a 1 M Na_2SO_4 electrolyte. Na^+ and SO_4^{2-} ions move in and out of the activated carbon pores during the storage and release of charge processes. Ion transport resistance and internal electrode resistance can cause the voltage response over time to become non-uniform during charging and discharging [20].

The electrode exhibited a discharge time of 195 s, indicating that the charge release process extended over most of the discharge period. This condition contributes to the electrode's ability to sustain charge release during testing [21]. During discharging, the voltage decreases sharply after the charging process ends. However, no noticeable IR drop was observed in the curve, indicating that voltage loss due to resistance was not a dominant response [22]. Consequently, most of the discharge time was spent releasing stored charge as the voltage decreased from approximately 1 V to near 0 V.

Based on the overall GCD curve, the *Moringa oleifera* leaves-based activated carbon electrode demonstrates the ability to store and release charge, with electrochemical performance indicated by a

capacitance of 130 F/g, an energy density of 18.06 Wh/kg, and a power density of 333.33 W/kg. These values confirm that the combination of the activated carbon's physical characteristics and the use of Na_2SO_4 can sustain gradual charge storage and release at a voltage of 1 V [23].

3.2.2. Cyclic Voltammetry Analysis

CV measurements were performed in order to examine how the *Moringa oleifera* leaves-based activated carbon electrode responds electrochemically within voltage ranges of 0-1 V and 0-2 V. These CV curves were used to observe changes in current as a function of voltage during charging and discharging. The shape and the area under the curves provide an indication of the electrode's charge storage response [24]. Therefore, changes in the curves across the two voltage windows were used as a basis for evaluating changes in the electrode's electrochemical performance. The electrochemical values were determined using Equation (2), Equation (3), and Equation (4):

$$C_{sp} = \frac{Q}{m\Delta V} \tag{2}$$

$$E_{sp} = \frac{1}{2}\frac{C_{sp}(\Delta V)^2}{3.6} \tag{3}$$

$$P_{sp} = \frac{E_{sp}\times 3600}{\Delta t} \tag{4}$$

where C_{sp} = mass-specific capacitance (F/g), E_{sp} = energy density (Wh/kg), P_{sp} = power density (W/kg), Q = stored charge (C), m = active mass (g), ΔV = voltage window (V), and Δt = discharge time (s) [25].

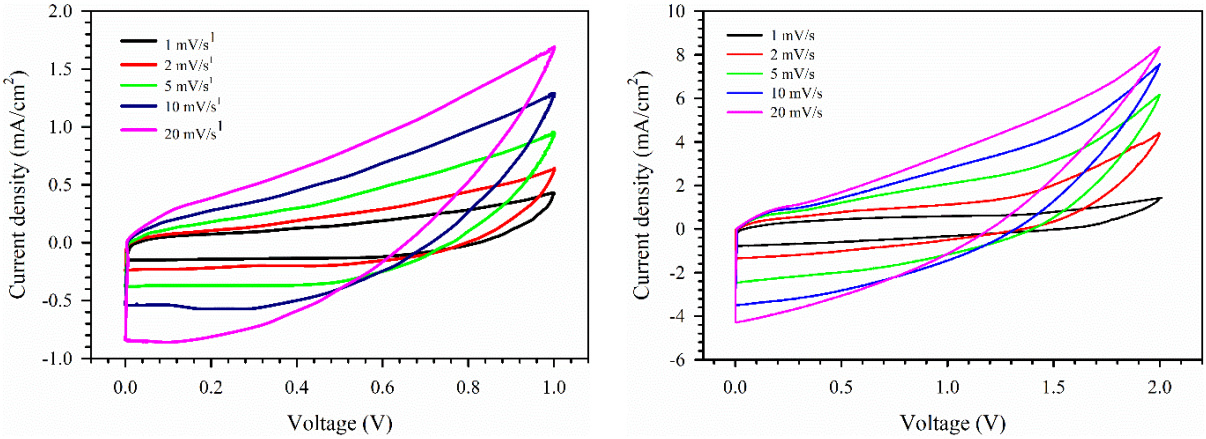


Figure 4. CV curves at voltage windows of (a) 1 V and (b) 2 V.

Figure 4 (a) shows the results of testing within a voltage window of 0 – 1 V at scan rates of 1, 2, 5, 10, and 20 mV/s. The curves at each scan rate exhibit shapes that tend to resemble the typical response of an electric double-layer capacitor (EDLC), although they do not form a perfect rectangle. This observation is consistent with the charge-storage characteristics reported for biomass-derived porous carbon electrodes [26]. At a scan rate of 1 mV/s, the capacitance was 45 F/g, the energy density was 6.25 Wh/kg, and the power density was 270 W/kg. When the scan rate was increased to 2, 5, 10, and 20 mV/s, the capacitance decreased to 35.8, 23.6, 16, and 9.91 F/g, respectively. The specific energy also decreased to 4.97, 3.28, 2.22, and 1.37 Wh/kg, respectively, while the specific power increased to 430, 710, 960, and 1,190 W/kg. Lower capacitance at higher scan rates has also been observed in biomass-derived activated carbon, indicating that changes in scan rate affect the electrode's charge storage response [27].

The electrochemical test results for the voltage window of 0 – 2 V, presented in Figure 4 (b), exhibit a similar trend in response to changes in scan rate. The curves within this voltage window have a larger area than those obtained from testing at 0 – 1 V. At 1 mV/s, the specific capacitance reached 153.33 F/g, the energy density reached 85.18 Wh/kg, and the power density reached 1,840 W/kg. When the scan rate was increased to 2, 5, 10, and 20 mV/s, the capacitance decreased to 133.33, 107, 69.33, and 37.58 F/g, respectively. The specific energy decreased to 74.07, 59.44, 38.51, and 20.87 Wh/kg, respectively, while the specific power increased to 3,200, 6,420, 8,320, and 9,020 W/kg. The lower capacitance observed at faster scan rates may be related to the reduced time available for electrolyte ions to reach the active sites of the electrode [24]. To further illustrate the effect of scan rate on the electrode's charge-storage performance, the relationship between specific capacitance and scan rate is presented in Figure 5.

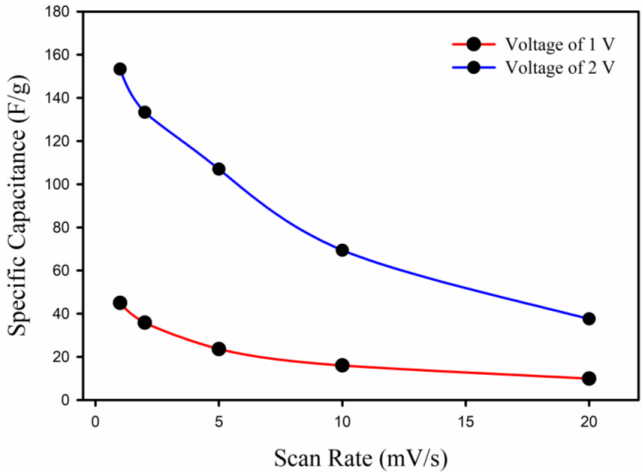


Figure 5. Specific capacitance as a function of scan rate at voltage windows of 0 – 1 V and 0 – 2 V.

Figure 5 provides a direct comparison of the capacitance response at the two voltage windows. The consistently higher values in the 0 – 2 V window indicate that the electrode delivers greater specific capacitance under this testing condition. The decrease in capacitance at higher scan rates is consistent with the limited time available for electrolyte ions to access the active sites within the electrode pores.

Testing using the 0 – 2 V range produced higher specific capacitance and specific energy values than testing using the 0 – 1 V range at all tested scan rates. At 1 mV/s, the specific capacitance increases from 45 F/g to 153.33 F/g, while the specific energy increases from 6.25 Wh/kg to 85.18 Wh/kg. The same trend was observed at scan rates of 2, 5, 10, and 20 mV/s, although the specific capacitance and specific energy values continued to decrease as the scan rate increased. Along with the increases in capacitance and specific energy, differences in current response between the two voltage windows were also observed in the CV curves in Figure 3 (a) and Figure 3 (b). The curve within the 0 – 1 V voltage window has a current density scale of approximately -1 mA/cm^2 to 2 mA/cm^2, whereas the scale within the 0 – 2 V voltage window ranges from approximately -6 mA/cm^2 to 10 mA/cm^2. The wider current density range in the 0 – 2 V test is associated with the larger potential window, which allows greater current variation during testing. This current response is also influenced by the capacitive characteristics of the electrode, as well as the ability of ions in the electrolyte to reach the electrode surface and pores. At faster scan rates, ions have less time to enter the electrode pores, which can reduce the measured capacitive response. The improvement in specific energy at the 0 – 2 V voltage window can be explained by the combined effects of the wider operating voltage and the higher specific capacitance obtained under this condition. For an ideal capacitive system, the stored energy is proportional to the specific capacitance and the square of the operating voltage [28]. Thus, a wider voltage range supports an increase in the measured specific capacitance value, which explains the energy storage capability of the *Moringa oleifera* leave-based supercapacitor electrodes obtained in this study. The relationship between specific energy and specific power is also presented in Figure 6 to further illustrate the energy-storage and power-delivery characteristics of the electrode.

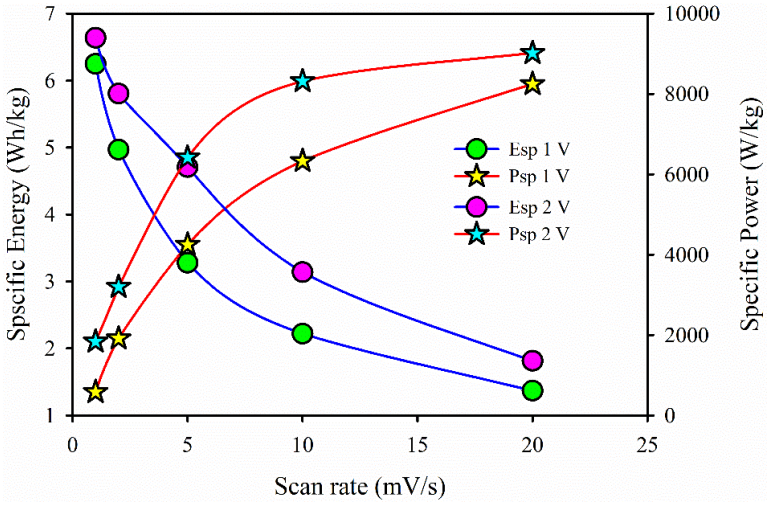


Figure 6. Ragone plot showing the relationship between specific energy and specific power at voltage windows of 0 – 1 V and 0 – 2 V.

Figure 6 illustrates the trade-off between energy storage and power delivery under the two voltage windows. For the 0 – 1 V window, the specific energy decreases from 6.25 Wh/kg to 1.37 Wh/kg as the specific power increases from 270 W/kg to 1,190 W/kg. Similarly, for the 0 – 2 V window, the specific energy decreases from 85.18 Wh/kg to 20.87 Wh/kg as the specific power increases from 1,840 W/kg to 9,020 W/kg. These results illustrate the relationship between the electrode's energy-storage capability and power delivery under different operating conditions.

From a practical perspective, these findings suggest that extending the operating voltage window to 0 – 2 V using aqueous 1 M Na_2SO_4 electrolyte can enhance the energy-storage capability of the H_3PO_4 activated *Moringa oleifera* leave waste-derived carbon electrode. The energy density of 85.18 Wh/kg, obtained at a scan rate of 1 mV/s, indicates promising energy-storage performance under the tested conditions; however, this value alone does not establish the performance of a practical supercapacitor device. It should be noted that operation at 0 – 2 V with an aqueous electrolyte may involve water decomposition and potential electrolyte instability; therefore, the electrochemical performance reported here should not be interpreted as confirmation of long-term stability at this voltage. Nevertheless, further investigations into cycling stability and long-term performance are needed to establish its suitability for practical supercapacitor devices.

Table 1. Electrochemical performance of various biomass-based supercapacitor electrodes.

Precusor	Voltage (V)	C_{sp} (F/g)	E_{sp} (Wh/kg)	P_{sp} (W/kg)	Reference
Peanut oil cake	2	300	15.89	493	[29]
Hemp hurd	2	105	38	761	[30]
Winery waste	2	32	17.7	303.42	[31]
Date stone	1.8	113.75	40.44	400	[32]
Coconut shell	2	88	48.9	1,000	[33]
Waste tea leaves	2	139.4	19.4	331.8	[34]
Moringa leaves	2	153.33	85.19	1,840	This research

Overall, the test results show that increasing the scan rate from 1 mV/s to 20 mV/s leads to lower specific capacitance and energy density, while increasing power density. Meanwhile, the use of a 0 – 2 V voltage window produces higher specific capacitance and specific energy values than the 0 – 1 V window. Thus, under the test conditions used, the 0 – 2 V voltage window provides greater energy storage capability, whereas higher scan rates have a more pronounced effect on increasing specific power. As shown in Table 1, the *Moringa oleifera* leave-derived activated carbon electrode exhibits the highest specific capacitance (153.33 F/g), specific energy (85.18 Wh/kg), and specific power (1,840 W/kg) among the biomass-derived electrodes listed.

4. CONCLUSION

This study successfully produced *Moringa oleifera* leaves-derived activated carbon by applying chemical activation with H_3PO_4, carbonizing the material in an N_2 atmosphere, followed by physical activation using CO_2. The thermal treatment resulted in a decrease in density from 0.94 g/cm^3 to 0.60 g/cm^3, representing a reduction of 36.17%. The electrochemical test results showed that the electrode exhibited charge-storage characteristics resembling those of an EDLC. For the 0 – 1 V voltage range, the specific capacitance values obtained using the CV and GCD methods were 45 F/g for CV and 130 F/g for GCD. Meanwhile, within the 0 – 2 V voltage window, CV testing yielded a capacitance of 153.33 F/g, an energy density of 85.18 Wh/kg, and a power density of 1,840 W/kg when the scan rate was 1 mV/s. Expanding the operating voltage range from 0 – 1 V to 0 – 2 V resulted in increased specific capacitance and specific energy in the CV test results, while increasing the scan rate led to decreases in specific capacitance and specific energy and an increase in specific power. The findings indicate that *Moringa oleifera* leaves-derived activated carbon has potential for supercapacitor electrode applications. Further studies are needed to evaluate its practical applicability beyond laboratory-scale testing.

AUTHOR CONTRIBUTIONS

Salma Safitri: Investigation, formal analysis, visualization, and writing—original draft. Fitriani Novalina Panjaitan: Investigation, organization, and data curation. Novi Yanti: Investigation, data processing, and formal analysis. Nursyafni Nursyafni: Validation, verification, and data curation. Apriwandi Apriwandi: Methodology, validation, and writing—review and editing. Rika Taslim: Research resources and manuscript review and editing. Erman Taer: Conceptualization, methodology, supervision, and manuscript review and editing. All authors approved the final manuscript and accepted accountability for their contributions.

FUNDING STATEMENT

This research was funded by Kemdiktisaintek, Republic of Indonesia, through the second-year Fundamental Research Scheme in 2026 (Contract No. 202/UN19.5.1.3/AL.04/2026).

DECLARATION OF AI USE

The authors declare that no AI tools were used in preparing this manuscript.

CONFLICT OF INTEREST

The authors declare no conflicts of interest.

DATA AVAILABILITY STATEMENT

All data supporting this study are included in the article. No separate datasets are available.

ETHICAL APPROVAL

Ethical approval was unnecessary, as no humans or animals were involved.

ACKNOWLEDGMENTS

This research was financially supported by the second-year 2026 Fundamental Research Scheme funded by the Directorate General of Higher Education (Kemdiktisaintek), Republic of Indonesia, through Contract No. 202/UN19.5.1.3/AL.04/2026.

REFERENCES

[1] Ren, J., Wang, Q., Xiang, Q., Yang, C., Liang, Y., Liu, J., Li, J., & Qian, D. (2023). Towards ultra-wide voltage window (3.2V) aqueous symmetric supercapacitors triggered by hybridizing FeNiCo oxides with Ni(pyrithione)$_2$ on FeNi foam. *Journal of Energy Storage*, **58**, 106338. DOI: https://doi.org/10.1016/j.est.2022.106338

[2] Gajewska, K., Moyseowicz, A., Minta, D., & Gryglewicz, G. (2023). Effect of electrolyte and carbon material on the electrochemical performance of high-voltage aqueous symmetric supercapacitors. *Journal of Materials Science*, **58**(4), 1721-1738.
DOI: https://doi.org/10.1007/s10853-023-08148-5

[3] Manasa, P., Sambasivam, S., & Ran, F. (2022). Recent progress on biomass waste derived activated carbon electrode materials for supercapacitors applications—A review. *Journal of Energy Storage*, **54**, 105290.
DOI: https://doi.org/10.1016/j.est.2022.105290

[4] Taer, E., Taslim, R., & Apriwandi, A. (2022). Biomass-based self-single-oxygen heteroatom-doped hierarchical porous carbon nanosheets for high-performance symmetrical supercapacitors. *ChemNanoMat*, **8**(8), e202200217.
DOI: https://doi.org/10.1002/cnma.202200217

[5] Taslim, R., Apriwandi, A., & Taer, E. (2022). Novel Moringa oleifera leaves 3D porous carbon-based electrode material as a high-performance EDLC supercapacitor. *ACS Omega*, **7**(41), 36489.
DOI: https://doi.org/10.1021/acsomega.2c04301

[6] Farma, R., Apriyani, I., Awitdrus, A., Taer, E., & Apriwandi, A. (2022). Hemicellulosa-derived Arenga pinnata bunches as free-standing carbon nanofiber membranes for electrode material supercapacitors. *Scientific Reports*, **12**(1), 2572.
DOI: https://doi.org/10.1038/s41598-022-06619-4

[7] Mendhe, A. & Panda, H. S. (2023). A review on electrolytes for supercapacitor device. *Discover Materials*, **3**(1), 29.
DOI: https://doi.org/10.1007/s43939-023-00065-3

[8] Fischer, J., Pohle, B., Dmitrieva, E., Thümmler, K., Fischer, S., & Mikhailova, D. (2022). Symmetric supercapacitors with cellulose-derived carbons and Na_2SO_4 electrolytes operating in a wide temperature range. *Journal of Energy Storage*, **55**, 105725.
DOI: https://doi.org/10.1016/j.est.2022.105725

[9] Ye, L., Feng, T., Kirk, D. W., & Jia, C. Q. (2024). Can aqueous Na2SO4-based neutral electrolyte increase energy density of monolithic wood biochar electrode supercapacitor?. *Energies*, **17**(15), 3710.
DOI: https://doi.org/10.3390/en17153710

[10] Krishnan, P., & Biju, V. (2022). Effect of electrolyte concentration on the electrochemical performance of RGO-Na_2SO_4 supercapacitor. *Materials Today: Proceedings*, **54**, 958-962.
DOI: https://doi.org/10.1016/j.matpr.2021.10.512

[11] Wu, X., Yang, H., Yu, M., Liu, J., & Li, S. (2021). Design principles of high-voltage aqueous supercapacitors. *Materials Today Energy*, **21**, 100739.
DOI: https://doi.org/10.1016/j.mtener.2021.100739

[12] Sabitov, A., Atamanov, M., Doszhanov, O., Saurykova, K., Tazhu, K., Kerimkulova, A., Orazbayev, A., & Doszhanov, Y. (2024). Surface characteristics of activated carbon sorbents obtained from biomass for cleaning oil-contaminated soils. *Molecules*, **29**(16), 3786.
DOI: https://doi.org/10.3390/molecules29163786

[13] Syguła, E., Ciolkosz, D., & Białowiec, A. (2024). The significance of structural components of lignocellulosic biomass on volatile organic compounds presence on biochar-a review. *Wood Science and Technology*, **58**(3), 859-886.
DOI: https://doi.org/10.1007/s00226-024-01557-y

[14] Khater, E. S., Bahnasawy, A., Hamouda, R., Sabahy, A., Abbas, W., & Morsy, O. M. (2024). Biochar production under different pyrolysis temperatures with different types of agricultural wastes. *Scientific Reports*, **14**(1), 2625.
DOI: https://doi.org/10.1038/s41598-024-52336-5

[15] Wang, Z., Xia, S., Ren, X., & Dong, Y. (2025). Phosphoric Acid Addition: Insight into the Mechanism Governing Biochar Structural Evolution. *Energies*, **18**(23), 6165.
DOI: https://doi.org/10.3390/en18236165

[16] Kayiwa, R., Kasedde, H., Lubwama, M., & Kirabira, J. B. (2021). Mesoporous activated carbon yielded from pre-leached cassava peels. *Bioresources and Bioprocessing*, **8**(1), 53.
DOI: https://doi.org/10.1186/s40643-021-00407-0

[17] Phothong, K., Tangsathitkulchai, C., & Lawtae, P. (2021). The analysis of pore development and formation of surface functional groups in bamboo-based activated carbon during CO_2 activation. *Molecules*, **26**(18), 5641.
DOI: https://doi.org/10.3390/molecules26185641

[18] Benoy, S. M., Hazarika, A., Rajbongshi, A., Bora, M., & Saikia, B. K. (2024). Hierarchical porous carbon derived from petroleum coke via one-step chemical activation for the fabrication of a supercapacitor and real time clock application. *RSC Advances*, **14**(30), 21411-21424.
DOI: https://doi.org/10.1039/d4ra03817g

[19] Klangvijit, K., Bowornthommatadsana, K., Phonyiem Reilly, M., Uwanno, T., Yordsri, V., Obata, M., Fujishige, M., Takeuchi, K., & Wongwiriyapan, W. (2025). Optimizing electrochemical performance: a study of aqueous electrolytes with hemp-derived activated carbon for supercapacitors. *ACS Omega*, **10**(7), 6601-6614.
DOI: https://doi.org/10.1021/acsomega.4c07518

[20] Abdulsalam, J., Otun, K., Gardee, N., Patel, B., Leswifi, T., & Mathe, M. K. (2023). Activated biocarbon from paper mill sludge as electrode material for supercapacitors: comparative performance evaluation in two aqueous electrolytes. *ACS Omega*, **8**(6), 5285.
DOI: https://doi.org/10.1021/acsomega.2c05887

[21] Zhang, X., Qiu, Z., Li, Q., Liang, L., Yang, X., Lu, S., Xiang, D. & Lai, F. (2022). Nickel acetate-assisted graphitization of porous activated carbon at low temperature for supercapacitors with high performances. *Frontiers in Chemistry*, **10**, 828381.
DOI: https://doi.org/10.3389/fchem.2022.828381

[22] Adam, R. A., Tarimo, D. J., Maphiri, V. M., Mirghni, A. A., Fasakin, O., & Manyala, N. (2025). Effects of the physisorption properties of human hair-derived activated carbon as a potential electrode for symmetric supercapacitor. *Materials for Renewable and Sustainable Energy*, **14**(1), 22.
DOI: https://doi.org/10.1007/s40243-024-00294-3

[23] Taslim, R., Refanza, R., Hamdy, M. I., Apriwandi, A., & Taer, E. (2023). One-step strategy of 3D hierarchical porous carbon with self-heteroatom-doped derived bread waste for high-performance supercapacitor. *Journal of Analytical and Applied Pyrolysis*, **171**, 105956.
DOI: https://doi.org/10.1016/j.jaap.2023.105956

[24] Farma, R., Julita, R. I., Apriyani, I., Awitdrus, A., & Taer, E. (2023). $ZnCl_2$-assisted synthesis of coffee bean bagasse-based activated carbon as a stable material for high-performance supercapacitors. *Materials Today: Proceedings*, **87**, 25-31.
DOI: https://doi.org/10.1016/j.matpr.2023.01.370

[25] Harahap, E. W., Taer, E., Rini, A. S., Taslim, R., & Apriwandi, A. (2022). Cassava peel derived self-doped and hierarchical porous carbon as an optimized electrode for the ultra-high energy density of supercapacitor. *Diamond and Related Materials*, **129**, 109407.
DOI: https://doi.org/10.1016/j.diamond.2022.109407

[26] Taer, E., Apriwandi, A., & Taslim, R. (2023). 3D meso-macroporous carbon derived spruce leaf biomass for excellent electrochemical symmetrical supercapacitor. *Materials Today: Proceedings*, **87**, 32-40.
DOI: https://doi.org/10.1016/j.matpr.2023.01.371

[27] Farma, R., Apriyani, I., Deraman, M., Taer, E., Setiadi, R. N., & Rini, A. S. (2023). Enhanced electrochemical performance of oxygen, nitrogen, and sulfur trial-doped *Nypa fruticans*-based carbon nanofiber for high performance supercapacitors. *Journal of Energy Storage*, **67**, 107611.
DOI: https://doi.org/10.1016/j.est.2023.107611

[28] Wang, Y., Duan, Y., Liang, X., Tang, L., Sun, L., Wang, R., Wei, S., Huang, H., Yang, P., & Hu, H. (2023). Hierarchical porous activated carbon derived from coconut shell for ultrahigh-performance supercapacitors. *Molecules*, **28**(20), 7187.
DOI: https://doi.org/10.3390/molecules28207187

[29] Ratnaji, T., Kennedy, L. J., & Vijaya, J. J. (2024). Peanut oil cake biomass-derived hierarchical porous carbon by dual step activation as potential electrodes for fabrication of prototype symmetric supercapacitor device. *International Journal of Energy Research*, **2024**(1), 4961636.
DOI: https://doi.org/10.1155/2024/4961636

[30] Minakshi, M., Mujeeb, A., Whale, J., Evans, R., Aughterson, R., Shinde, P. A., Ariga, K., & Shrestha, L. K. (2024). Synthesis of porous carbon honeycomb structures derived from hemp for hybrid supercapacitors with improved electrochemistry. *ChemPlusChem*, **89**(12), e202400408.
DOI: https://doi.org/10.1002/cplu.202400408

[31] Tyagaraj, H. B., Mahamiya, V., Marje, S. J., Safarkhani, M., SK, G., Al-Hajri, E., Chodankar, N. R., Huh, Y. S., & Han, Y. K. (2024). Waste-to-energy material: Winery-waste derived heteroatoms containing graphene-like porous carbon for high-voltage supercapacitor. *Materials Today Sustainability*, **27**, 100901.
DOI: https://doi.org/10.1016/j.mtsust.2024.100901

[32] Shuaibu, A. D., Mirghni, A. A., Shah, S. S., Alzahrani, A. S., & Aziz, M. A. (2026). All-biomass electrochemical supercapacitors cell utilizing date stone-derived activated carbon electrodes and cellulose hydrogel electrolyte. *Next Energy*, **11**, 100555.
DOI: https://doi.org/10.1016/j.nxener.2026.100555

[33] Lee, K. C., Lim, M. S. W., Hong, Z. Y., Chong, S., Tiong, T. J., Pan, G. T., & Huang, C. M. (2021). Coconut shell-derived activated carbon for high-performance solid-state supercapacitors. *Energies*, **14**(15), 4546.
DOI: https://doi.org/10.3390/en14154546

[34] Bhat, M. Y., Khan, F., Ayoub, Z., Jain, A., & Gull, S. (2025). Recycling biowaste into energy storage: waste tea leaves-derived hierarchical porous activated carbon for supercapacitors. *Journal of Power Sources*, **655**, 237969.
DOI: https://doi.org/10.1016/j.jpowsour.2025.237969